Local and Nonlocal Parallel Heat Transport in General Magnetic Fields

D. del-Castillo-Negrete* and L. Chacón

Oak Ridge National Laboratory, Oak Ridge, Tennessee 37831-8071, USA

(Received 26 July 2010; published 11 May 2011)

A novel approach for the study of parallel transport in magnetized plasmas is presented. The method avoids numerical pollution issues of grid-based formulations and applies to integrable and chaotic magnetic fields with local or nonlocal parallel closures. In weakly chaotic fields, the method gives the fractal structure of the devil's staircase radial temperature profile. In fully chaotic fields, the temperature exhibits self-similar spatiotemporal evolution with a stretched-exponential scaling function for local closures and an algebraically decaying one for nonlocal closures. It is shown that, for both closures, the effective radial heat transport is incompatible with the quasilinear diffusion model.

DOI: 10.1103/PhysRevLett.106.195004 PACS numbers: 52.25.Fi, 02.70.−c, 52.25.Xz, 52.65.−y

The study of transport in magnetized plasmas is a problem of fundamental interest in controlled fusion, space plasmas, and astrophysics research. Three issues make this problem particularly challenging: (i) the extreme anisotropy between the parallel (i.e., along the magnetic field), $\chi_\parallel$, and the perpendicular, $\chi_\perp$, conductivities ($\chi_\parallel/\chi_\perp$ may exceed 10^{10} in fusion plasmas); (ii) magnetic *field-line chaos* which in general complicates (and may preclude) the construction of magnetic field-line coordinates, and (iii) nonlocal parallel transport in the limit of small collisionality. As a result of these challenges, standard finite-difference and finite-element numerical methods suffer from a number of ailments including the pollution of perpendicular dynamics due to truncation errors in the discretization, the lack of a discrete maximum principle, and potentially insurmountable problems in the inversion of the discretized equation due to singularities of the parallel transport operator [1]. Previous work partially addressing some of these issues include finite-element numerical implementation of nonlocal heat transport [2], the use of high-order discretizations to mitigate numerical pollution in finite-difference [3,4] and finite-element methods [4,5], the use of limiters at the discrete level in finite differences [6] and finite elements [7] to enforce a maximum principle, and the use of ''ghost surfaces'' in steady-state solutions [8,9].

Motivated by the strong anisotropy typically encountered in magnetized plasmas ($\chi_\parallel/\chi_\perp \sim 10^{10}$), we study parallel heat transport in the extreme anisotropic regime $\chi_\perp = 0$. To overcome the numerical and algorithmic challenges discussed above, we present a novel Lagrangian Green's function approach. The proposed method bypasses the need to discretize and invert the transport operators on a grid and allows the integration of the parallel transport equation without perpendicular pollution, while preserving the positivity of the temperature field at all times. The method is applicable to local and nonlocal transport in integrable or chaotic magnetic fields.

As an application, we study radial heat transport in cylindrical geometry in weakly chaotic and fully chaotic magnetic fields. The weakly chaotic case is presented to illustrate the accuracy of the method. Going beyond previous studies [8], we unveil the fractal structure of the devil's staircase in the previously inaccessible $\chi_\perp = 0$ regime. This result opens the possibility of a deeper understanding of the role of cantori which have been observed to act as partial transport barriers in numerical studies [8,9] and experiments [10]. The second application pertains to the study of heat transport in fully chaotic fields. This has been a problem of considerable interest in fusion and astrophysical plasmas since the pioneering work in Refs. [11,12]. Here, we present novel results on the self-similar spatiotemporal evolution of the radial temperature profile and show that, contrary to what is typically assumed in transport studies, the effective radial transport is not diffusive. In particular, transport does not adhere to the Fourier-Fick prescription that assumes a local linear relation between the radial heat flux and the radial temperature gradient.

Our starting point is the heat transport equation in a constant-density plasma

$$\partial_t T = -\nabla \cdot \mathbf{q}, \tag{1}$$

where $\mathbf{q}$ is the heat flux. For local transport, in the limit $\chi_\perp = 0$, $\mathbf{q} = -\chi_\parallel[\hat{\mathbf{b}} \cdot \nabla T]\hat{\mathbf{b}}$, where $\hat{\mathbf{b}} = \mathbf{B}/|B|$. Substituting this flux into (1), we get $\partial_t T = -\partial_s q_\parallel$, $q_\parallel = -\chi_\parallel \partial_s T$, where $\partial_s = \hat{\mathbf{b}} \cdot \nabla$ is the derivative along the field line, and we have assumed the tokamak ordering $\partial_s \ln B \approx 0$. For nonlocal transport, we follow Refs. [2,13,14] and consider the closure

$$q_\parallel = -\frac{\chi_\parallel}{\pi} \int_0^\infty \frac{T(s+z) - T(s-z)}{z} dz. \tag{2}$$

In Fourier space, both transport models can be written in the particularly compact form

$$\partial_t \hat{T} = -\chi_\parallel |k|^\alpha \hat{T}, \tag{3}$$

where $\hat{T}$ is the Fourier transform of T. For the local closure, $\alpha = 2$, whereas for the nonlocal closure in Eq. (2), $\alpha = 1$.

In principle, $\chi_\parallel$ can have a spatial dependence, but it must be constant along field lines, i.e., $\partial_s \chi_\parallel = 0$.

The proposed method is based on the Green's function solution of Eq. (3) along the magnetic field. The unique magnetic field-line trajectory $\mathbf{r}(s)$ (parametrized by the arc length s) that goes through a point $\mathbf{r}_p$ is given by the solution of $\frac{d\mathbf{r}}{ds} = \hat{\mathbf{b}}$, $\mathbf{r}(s=0) = \mathbf{r}_p$. Thus, given an initial condition in the whole domain, $T(\mathbf{r}, t=0)$, the temperature at $\mathbf{r} = \mathbf{r}_p$ at time t is given by

$$T(\mathbf{r}_p, t) = \int_{s_1}^{s_2} T_0[\mathbf{r}(s)] G_\alpha(s, t) ds, \tag{4}$$

where $T_0[\mathbf{r}(s)] = T[\mathbf{r}(s), t=0]$ is the initial condition along the field line. G_α is the Green's function defined as the solution of the initial value problem of Eq. (3) for a Dirac delta function initial condition in space. For unbounded field lines $[(s_1, s_2) = (-\infty, \infty)]$, the Green's function is given by

$$G_\alpha(s, t) = \frac{1}{2\pi} \int_{-\infty}^{\infty} e^{-\chi_\parallel t |k|^\alpha - iks} dk. \tag{5}$$

For $\alpha = 2$ (local transport), Eq. (5) gives the Gaussian distribution

$$G_2(s, t) = \frac{1}{2\sqrt{\pi}} (\chi_\parallel t)^{-1/2} \exp\left[-\frac{s^2}{4\chi_\parallel t} \right], \tag{6}$$

and for $\alpha = 1$ (nonlocal, free-streaming transport), it gives the Cauchy distribution

$$G_1(s, t) = \frac{(\chi_\parallel t)^{-1}}{\pi} \frac{1}{1 + (s/\chi_\parallel t)^2}. \tag{7}$$

For $1 < \alpha < 2$, $G_\alpha = (\chi_\parallel t)^{-1/\alpha} K_{\alpha,0}[(\chi_\parallel t)^{-1/\alpha} s]$, where $K_{\alpha,0}$ is the symmetric α-stable Levy distribution [15]. For more general closures [2,14], the Green's function must be computed numerically. Here we limit attention to unbounded field lines. However, transport along bounded lines, including periodic lines in two and three dimensions or lines intersecting boundaries, can also be studied with the appropriate Green's function. The numerical integration of the field-line trajectories was done by using the high-order adaptive ordinary differential equation solver ODEPACK. We have thoroughly verified the numerical implementation against analytical solutions.

At this point, it is important to indicate a fundamental difference between our work and the numerical implementation of the nonlocal closure discussed in Refs. [2,14]. In these references, the flux is calculated by integrating the transport kernel along the field lines. But, once the flux is computed, the Lagrangian approach is abandoned and the flux is mapped to Gaussian quadrature points for the finite-element standard integration of the temperature evolution equation on a grid. In contrast, in the method proposed here, the assumption $\chi_\perp = 0$ allows the use of a fully Lagrangian approach that completely bypasses the use of finite differences or finite elements, thus circumventing the numerical issues discussed earlier.

We assume a periodic, straight cylinder configuration of length $L = 2\pi R$ with $R = 5$. The magnetic field consists of a perturbed tokamaklike equilibrium of the form $\mathbf{B} = (rB/\lambda)/[1 + (r/\lambda)^2]\hat{\mathbf{e}}_\theta + B_0 \hat{\mathbf{e}}_z + \mathbf{B}_1(r, \theta, z)$ with a monotonic q, $B_0 = 1$, and $B/B_0 = 10^{-1}$. To fit a spectrum of resonant modes with n/m ranging from $4/5$ to $1/5$, we choose λ so that $q_{\min} = 1.24 \approx 5/4$ and $q_{\max} = 5$. The magnetic potential of the perturbation, $\mathbf{B}_1 = \nabla \times A_z \hat{\mathbf{e}}_z$, consists of a superposition of modes $A_z(r, \theta, z) = \sum_{m,n} A_{mn}(r) \cos(m\theta - nz/R + \zeta_{mn})$, with

$$A_{mn} = \epsilon a(r) \left(\frac{r}{r_*} \right)^m \exp\left[\left(\frac{r_* - r_0}{\sqrt{2}\sigma} \right)^2 - \left(\frac{r - r_0}{\sqrt{2}\sigma} \right)^2 \right], \tag{8}$$

$\epsilon = 10^{-4}$, and $\sigma = 0.5$. For each (m, n), the values of r_* and r_0 are chosen so that the safety factor satisfies $q(r_*) = m/n$ and $dA_{mn}/dr(r = r_*) = 0$. The prefactor $(r/r_*)^m$ is included to guarantee the regularity of the radial eigenfunction near the origin, $r \sim 0$. The function $a(r) = \{1 - \tanh[(r-1)/0.05]\}/2$ is introduced to guarantee the perturbation to vanish at $r = 1$ and thus the existence of well-defined flux surfaces at the plasma boundary.

In the study of transport in weakly chaotic fields, only two modes $(m, n) = (5, 2), (4, 1)$ were included. As the Poincaré plot in Fig. 1 shows, in this case the magnetic field exhibits a rich fractal-like structure resulting from the existence of higher-order resonances. In this and all the subsequent results, $\psi = r^2/(2R^2)$ denotes the radial flux coordinate. As discussed in Refs. [8,9,16], weakly chaotic fields give rise to devil's staircase temperature profiles in which higher-order resonances lead to flat spots in the profile, while Kolmogorov-Arnold-Moser invariant circles and cantori lead to strong gradients. Our numerical method is able to find an accurate solution of the radial temperature profile at arbitrary radial resolutions. To illustrate this, we show in Fig. 2 the fractal structure of devil's staircase in the previously inaccessible limit $\chi_\parallel/\chi_\perp \to \infty$. The plots shows the time-asymptotic, radial temperature profile along the $\theta = 2.7$ horizontal line in Fig. 1, corresponding to the initial condition $T_0 = 1 - 2R^2\psi$. Note that the steady state is the same in the local and the nonlocal cases. This is because, asymptotically, both transport operators enforce constant temperature along field lines.

To study transport in a fully chaotic magnetic field, we consider a set of 21 strongly overlapping modes. In this case, the Poincaré plot (not shown) is fully hyperbolic and does not exhibit any structure. The initial condition consists of a narrow "cylindrical shell" of the form $T_0 = \exp[-R^2(\psi - \psi_0)^2/\sigma^2]$, with $\psi_0 = 0.18$ and $\sigma = 0.05$. Figure 3 shows the time evolution of the radial profile of the temperature averaged in θ and z, $\langle T \rangle$, in the local and the nonlocal (free-streaming) regimes. In both regimes, the temperature exhibits an asymptotic self-similar evolution of the form $\langle T \rangle(\psi, t) = (\chi_\parallel t)^{-\gamma/2} L(\eta)$, where the similarity variable is defined as $\eta = (\psi - \psi_0)/(\chi_\parallel t)^{\gamma/2}$, with γ the scaling exponent. From here, it follows

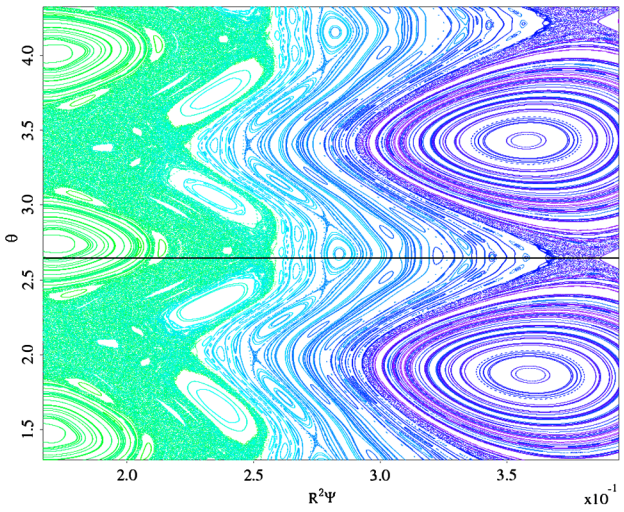

FIG. 1 (color online). Poincaré plot of the weakly chaotic magnetic field used in the solution of the parallel heat transport equation shown in Fig. 2.

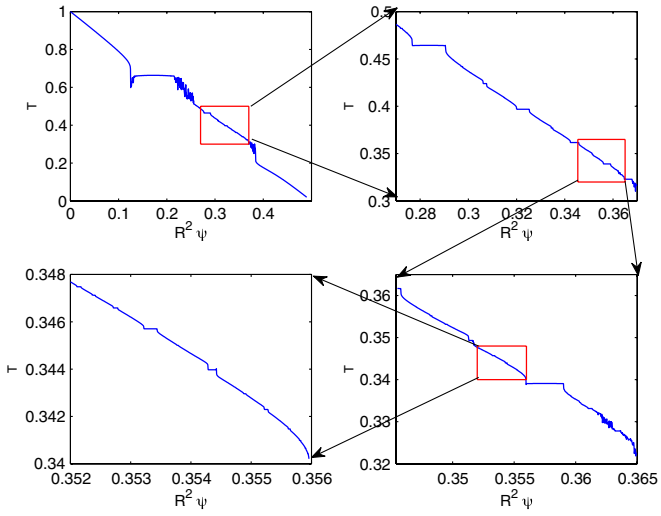

FIG. 2 (color online). Radial temperature profile of the time-asymptotic solution of the parallel heat transport equation for the weakly chaotic magnetic field in Fig. 1. The zooms in the successive panels unveil the fractal structure of the devil's staircase profile.

that the second moment scales as $\bar{\psi}^2 \sim t^\gamma$. Consistently with Refs. [11,12], we find subdiffusive scaling ($\gamma = 1/2$) in the case of local transport ($\alpha = 2$) and diffusive scaling ($\gamma = 1$) in the case of free streaming ($\alpha = 1$). However, the study of the properties of the scaling function provides important transport information beyond the scaling of the second moment. As Fig. 3 shows, for local parallel transport the scaling function is a stretched exponential. In contrast, the scaling function in the nonlocal case is strongly non-Gaussian and exhibits an algebraic decay.

A key issue in the study of heat transport in magnetically confined plasmas is to understand the effective radial energy transport, which ultimately determines the energy confinement time of the system. Within the standard diffusion paradigm, the study of radial transport is based on the Fourier-Fick prescription. This prescription assumes that the radial heat flux and the radial temperature gradient, averaged over z and θ, satisfy $\langle \mathbf{q} \cdot \hat{e}_\psi \rangle = -\chi_{\text{eff}} \langle \nabla T \cdot \hat{e}_\psi \rangle$, where $\hat{e}_\psi = \hat{e}_r$ is the unit vector in the radial direction. Although this prescription is used to model a wide range of transport problems, recent studies have questioned its validity in the presence of nondiffusive and nonlocal transport phenomena (see, for example, Refs. [15,17,18], and references therein). In fact, in what follows, we show that, unless one incorporates unphysical spatiotemporal dependencies in χ_{eff}, the effective radial heat transport resulting from parallel transport in fully stochastic 3D magnetic fields is inconsistent with the local diffusion assumption. Our approach is based on the comparison

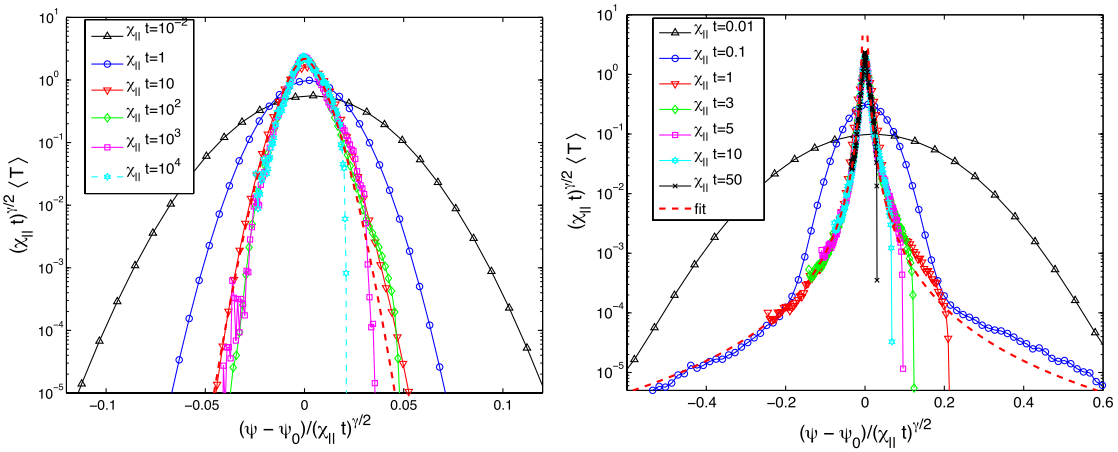

FIG. 3 (color online). Self-similar spatiotemporal evolution of the radial temperature profile in a fully chaotic magnetic field. The left panel shows the local transport ($\alpha = 2$) case with subdiffusive scaling exponent $\gamma = 1/2$. The dashed line denotes a stretched-exponential fit $L \sim \exp[-(|\eta|/\mu)^\nu]$ with $\nu \approx 1.6$ and $\mu \approx 0.0095$. The right panel shows the nonlocal transport ($\alpha = 1$) case with diffusive scaling exponent $\gamma = 1$. In this case, the scaling function is strongly non-Gaussian and, as the dashed-line fit shows, it exhibits algebraic decay of the form $L \sim \eta^{-3}$.

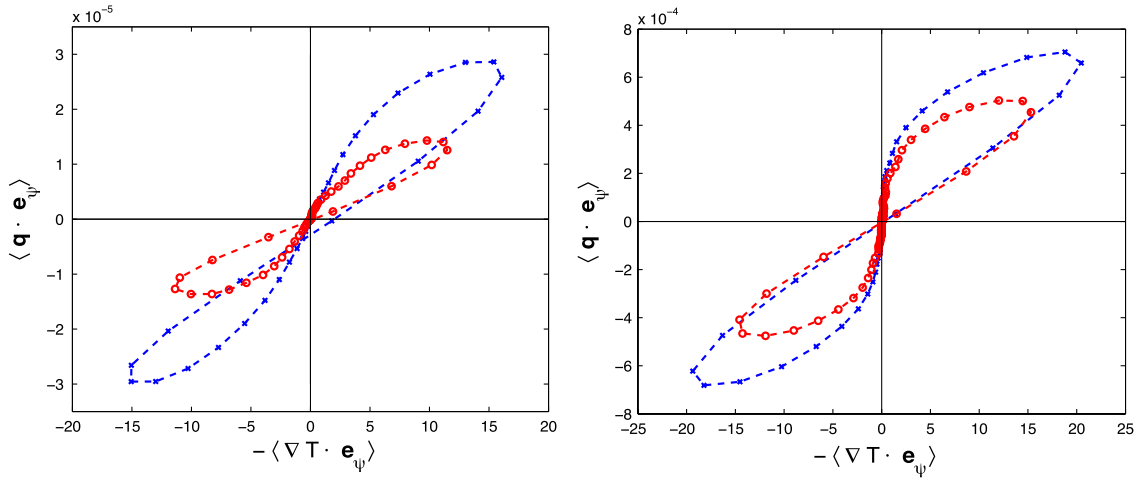

FIG. 4 (color online). Flux-gradient parametric curves obtained from the numerical integration of the parallel heat transport equation in a fully chaotic magnetic field. The left panel corresponds to the local transport ($\alpha = 2$) solutions shown in Fig. 3 for $\chi_\parallel t = 80$ (dashed-crosses line) and $\chi_\parallel t = 200$ (dashed-circles line). The right panel corresponds to the free-streaming transport ($\alpha = 1$) solutions shown in Fig. 3 for $\chi_\parallel t = 4$ (dashed-crosses line) and $\chi_\parallel t = 8$ (dashed-circles line).

between the temperature gradient $\langle \nabla T \cdot \hat{e}_\psi \rangle$ and the heat flux $\langle \mathbf{q} \cdot \hat{e}_\psi \rangle$, both of which are computed directly from the solutions $\langle T \rangle$ of the parallel heat transport equation shown in Fig. 3. The flux as a function of ψ is obtained from $\langle \mathbf{q} \cdot \hat{e}_\psi \rangle = -(1/\sqrt{2\psi}) \frac{d}{dt} \int_0^\psi \langle T \rangle d\psi'$, which follows from Eq. (1), and the gradient $\langle \nabla T \cdot \hat{e}_\psi \rangle = \sqrt{2\psi} \partial_\psi \langle T \rangle$. Figure 4 shows the parametric curves $\mathcal{C}(\psi) = [-\langle \nabla T \cdot \hat{e}_\psi \rangle(\psi), \langle \mathbf{q} \cdot \hat{e}_\psi \rangle(\psi)]$ tracing the values of the flux and the gradient as functions of ψ in the flux-gradient plane. In both the diffusive $\alpha = 2$ and the free-streaming $\alpha = 1$ cases, the flux-gradient parametric curves exhibit two key features: (i) The flux is a multivalued function of the gradient (i.e., the curves exhibit "loops"), and (ii) the shape of the curves depends on time. In the case of a constant (in space and time) diffusivity χ_{eff}, the local diffusion assumption requires the parametric curves to be straight lines. The only way to make the local diffusion assumption consistent with a multivalued flux-gradient relation is to incorporate an *ad hoc* spatial dependence in χ_{eff}. Similarly, the only way to explain the temporal variation of the flux-gradient curves is to incorporate an *ad hoc* temporal dependence in χ_{eff}. Although, formally, one could construct these spatiotemporal diffusivities to fit the data, such dependencies are inconsistent with the physics of the problem because the magnetic field is time-independent, and the field-line chaos is uniform in ψ by construction. This implies that the effective radial heat transport due to parallel transport in fully chaotic magnetic fields is incompatible with the quasilinear diffusion transport model.

This work was sponsored by the Office of Applied Scientific Computing Research and the Office of Fusion Energy Sciences of the U.S. Department of Energy at Oak Ridge National Laboratory, managed by UT-Battelle, LLC, for the U.S. Department of Energy under Contract No. DE-AC05-00OR22725.

*delcastillod@ornl.gov

[1] S. R. Hudson, Phys. Plasmas **17**, 114501 (2010).
[2] E. D. Held, J. D. Callen, C. C. Hegna, C. R. Sovinec, T. A. Gianakon, and S. E. Kruger, Phys. Plasmas **11**, 2419 (2004).
[3] S. Guenter, Q. Yu, J. Kruger, and K. Lackner, J. Comput. Phys. **209**, 354 (2005).
[4] S. Guenter, K. Lackner, and C. Tichmann, J. Comput. Phys. **226**, 2306 (2007).
[5] C. R. Sovinec, A. H. Glasser, T. A. Gianakon, D. C. Barnes, R. A. Nebel, S. E. Kruger, D. D. Schnack, S. J. Plimpton, A. Tarditi, and M. S. Chu, J. Comput. Phys. **195**, 355 (2004).
[6] P. Sharma and G. W. Hammett, J. Comput. Phys. **227**, 123 (2007).
[7] D. Kuzmin, M. J. Shashkov, and D. Svyatskiy, J. Comput. Phys. **228**, 3448 (2009).
[8] S. R. Hudson and J. Breslau, Phys. Rev. Lett. **100**, 095001 (2008).
[9] S. R. Hudson, Phys. Plasmas **16**, 010701 (2009).
[10] R. Lorenzini *et al.*, Nature Phys. **5**, 570 (2009).
[11] J. R. Jokipii and E. N. Parker, Phys. Rev. Lett. **21**, 44 (1968).
[12] A. B. Rechester and M. N. Rosenbluth, Phys. Rev. Lett. **40**, 38 (1978).
[13] G. W. Hammett and F. W. Perkins, Phys. Rev. Lett. **64**, 3019 (1990).
[14] E. D. Held, J. D. Callen, C. C. Hegna, and C. R. Sovinec, Phys. Plasmas **8**, 1171 (2001).
[15] D. del-Castillo-Negrete, B. A. Carreras, and V. Lynch, Phys. Plasmas **11**, 3854 (2004).
[16] S. R. Hudson, Phys. Rev. E **76**, 046211 (2007).
[17] D. del-Castillo-Negrete, Phys. Plasmas **13**, 082308 (2006).
[18] D. del-Castillo-Negrete, P. Mantica, V. Naulin, and J. J. Rasmussen, Nucl. Fusion **48**, 075009 (2008).